

# Special and General Relativistic Effects in Galactic Rotation Curves

Alan Cooney, Dimitrios Psaltis, Dennis Zaritsky  
*Steward Observatory and Department of Physics,  
University of Arizona, 933 N. Cherry Ave, Tucson, AZ 85721, USA*  
(Dated: February 15, 2012)

The observed flat rotation curves of galaxies require either the presence of dark matter in Newtonian gravitational potentials or a significant modification to the theory of gravity at galactic scales. Detecting relativistic Doppler shifts and gravitational effects in the rotation curves offers a tool for distinguishing between predictions of gravity theories that modify the inertia of particles and those that modify the field equations. These higher-order effects also allow us in principle, to test whether dark matter particles obey the equivalence principle. We calculate here the magnitudes of the relativistic Doppler and gravitational shifts expected in realistic models of galaxies in a general metric theory of gravity. We identify a number of observable quantities that measure independently the special- and general-relativistic effects in each galaxy and suggest that both effects might be detected in a statistical sense by combining appropriately the rotation curves of a large number of galaxies.

## I. INTRODUCTION

The rotation curves of galaxies are direct probes of the shape of their gravitational fields and their matter content. That the inferred circular velocities remain approximately constant, even at large distances from the central luminous matter, is the strongest evidence for the presence of dark matter at galactic scales [1].

Despite its simplicity and remarkable success in accounting for observations over a wide range of scales, explaining galactic rotation curves with dark matter remains a hypothesis; to date the candidate dark matter particles have eluded direct detection [2]. In the meantime, several possible modifications to the theory of gravity have been explored in attempts to explain the observed galactic rotation curves. The MODified Newtonian Dynamics (MOND) framework has been the most successful attempt phenomenologically [3, 4], but suffers from the fact that it is not relativistic. As a result, it cannot be used in its empirical form to generate predictions for gravitational lensing or for the dynamical evolution of systems at scales comparable to the Hubble scale.

Earlier [5] attempts to develop a relativistic theory of gravity that mimics the MOND phenomenology often faced fundamental difficulties, such as problems with causality or inadequacies in accounting for gravitational lensing in galaxies. More recently, new models [6] have been developed to resolve these difficulties, but they introduce several additional fields and auxiliary functions. Such additions negate the most appealing aspect of the original MOND, i.e., that galactic rotation curves and the Tully-Fisher relation were accounted for with the introduction of a single acceleration scale.

Most previous attempts aim to reproduce the MOND phenomenology by modifying the general relativistic field equations. However, in principle, the MOND phenomenology can also be achieved in the non-relativistic limit by modifying the equivalence principle, i.e., the inertia of test particles [7]. Which of the two aspects of the theory of gravity need to be altered in order to account for the observed rotation curves of galaxies, in the absence of dark matter? This question cannot be resolved solely with observations of the non-relativistic Doppler shifts of tracer particles. Ideas involving violations of the equivalence principle have been tested empirically, within the dark matter interpretation of galactic rotation curves [8], but not in the framework of modified gravity.

In this article, we aim to address this question by calculating the second order special- and general-relativistic corrections to the Doppler shifts of atomic lines used to infer the rotation curves of galaxies. Similar calculations in General Relativity, as well as strategies for using such measurements to map the spacetimes of galaxies have been reported in previous studies [9]. Here we focus only on the second-order effects and evaluate them using only the symmetries of the spacetime. More importantly, we show explicitly that, if the underlying theory of gravity obeys the equivalence principle, then the second-order effects can be determined entirely using knowledge of the non-relativistic Doppler shifts and without any assumptions regarding the underlying field equations of the theory. As a result, the relation between non-relativistic and relativistic effects can be used as a test of the equivalence principle at galactic scales, independent of whether dark matter or modified gravitational field equations are responsible for the flat rotation curves.

## II. PARTICLES AND PHOTONS IN GALACTIC POTENTIALS

### A. The Circular Orbits of Particles

We begin by assuming that the gravitational potential of a galaxy exhibits a high degree of axisymmetry. We will ultimately calculate the second-order Doppler shifts and the gravitational corrections assuming that the spacetime of each galaxy is asymptotically flat. This approach is formally appropriate only for a galaxy in an otherwise empty Universe; in a subsequent section, we correct for the Cosmological redshift of the galaxy.

Our assumptions motivate our choice of metric

$$ds^2 = g_{tt}(r, \theta) dt^2 + 2g_{t\phi}(r, \theta) dt d\phi + g_{rr}(r, \theta) dr^2 + g_{\theta\theta}(r, \theta) d\theta^2 + r^2 \sin^2 \theta d\phi^2, \quad (1)$$

where  $g_{tt}$ ,  $g_{t\phi}$ ,  $g_{rr}$ , and  $g_{\theta\theta}$  are undetermined functions of the coordinate radius  $r$  and the polar angle  $\theta$ . The  $g_{t\phi}$  coefficient is associated with frame-dragging, which we expect not to be significant for galaxies and will be neglected henceforth. For comparison, we recall that in General Relativity, the external spacetime of a spherically symmetric object is unique and is given by the Schwarzschild solution, for which  $g_{t\phi} = 0$ ,  $g_{\theta\theta} = r^2$  and,

$$g_{tt} = g_{rr}^{-1} = \left(1 - \frac{2GM}{rc^2}\right). \quad (2)$$

Here  $G$  is the gravitational constant and  $M$  is the gravitational mass of the object. Because of the assumption of the validity of the equivalence principle, matter and photons follow geodesics in the spacetime described by the metric (1).

We describe the motion of a massive particle in terms of its 4-velocity  $u^\mu \equiv (u^t, u^r, u^\theta, u^\phi)$ . We choose our coordinate system so that the orbit of the particles we study will lie on the equatorial plane, i.e., we will set  $\sin \theta = 1$  and  $u^\theta = 0$ . The requirement  $u_\mu u^\mu = -1$  for the 4-velocity of a massive particle leads to the constraint

$$g_{tt} (u^t)^2 + g_{rr} (u^r)^2 + r^2 (u^\phi)^2 = -1. \quad (3)$$

For a particle in a circular orbit at coordinate radius  $r_e$ , we require that the radial component of its 4-velocity is zero, which makes equation (3) a constraint on  $u^t$  and  $u^\phi$ . This constraint is also true for the turning points in an elliptical orbit. What sets a circular orbit apart is the fact that all points in the trajectory are turning points, i.e., that

$$\frac{du^r}{dr} = 0, \quad (4)$$

which specifies the  $u^t$  component of the 4-velocity uniquely

$$g_{tt} (u^t)^2 \left(1 - \frac{1}{2} \frac{d \ln |g_{tt}|}{d \ln r}\right) = -1. \quad (5)$$

We can use expression (3) to solve for the  $u^\phi$  component of the 4-velocity. Whatever our theory of gravity is, we expect that the outer regions of the galaxies are in the weak field, so we can find an approximation to the desired accuracy by expanding our metric away from the flat solution

$$g_{tt} = -1 + \epsilon^2 g_{tt}^{(2)} + \mathcal{O}(\epsilon)^3, \quad (6)$$

where we have introduced  $\epsilon$  merely as a dummy parameter that allows us to keep track of the expansion order. We denote the leading order correction to the metric element as  $\epsilon^2$ , because we are counting orders in terms of the expansion of the velocity, which will be proportional to the square root of  $g_{tt}^{(2)}$ . Using relations (3)–(6), we obtain that the components of the 4-velocity of a particle in a circular orbit are

$$u^t = 1 + \epsilon^2 \left[ \frac{1}{2} \left( g_{tt}^{(2)} - \frac{1}{2} \frac{d g_{tt}^{(2)}}{d \ln r} \right) \right] + \mathcal{O}(\epsilon)^3, \quad (7)$$

$$u^r = 0, \quad (8)$$

$$u^\theta = 0, \quad (9)$$

$$u^\phi = \epsilon \left[ \frac{1}{r} \sqrt{-\frac{1}{2} \frac{d g_{tt}^{(2)}}{d \ln r}} \right] + \mathcal{O}(\epsilon)^3. \quad (10)$$

We emphasize that the components of the 4-velocity of the particle in circular orbit depend only on the value and the local radial derivative of the  $g_{tt}$  element of the metric.

For comparison, in a Schwarzschild metric, the non-zero components of the 4-velocity of a particle in a circular orbit are given by

$$u^t \simeq 1 + 3 \frac{GM}{r} \quad (11)$$

$$u^\phi \simeq \frac{1}{r} \left( \frac{GM}{r} \right)^{1/2}. \quad (12)$$

## B. The Redshift of Photons

Our next goal is to calculate the trajectories and energy shifts of photons as they propagate from their origin in the galaxy to a distant observer. For a photon with 4-momentum  $k^\mu = (k^t, k^r, k^\theta, k^\phi)$ , there are conservation laws that arise from the two Killing vectors  $\xi^\mu = (1, 0, 0, 0)$  and  $\eta^\mu = (0, 0, 0, 1)$  of the spacetime, namely the conservation of energy

$$\varepsilon_p \equiv -g_{\mu\nu} k^\mu \xi^\nu = -g_{tt} k^t \quad (13)$$

and of angular momentum

$$l_p \equiv g_{\mu\nu} k^\mu \eta^\nu = r^2 k^\phi. \quad (14)$$

In its trajectory, the photon experiences an overall redshift and Doppler shift, which is given by

$$1 + z \equiv \frac{\nu_e}{\nu_{\text{obs}}} = \frac{g_{\mu\nu}(r_e) u_e^\mu k_e^\nu}{g_{\mu\nu}(r_{\text{obs}}) u_{\text{obs}}^\mu k_{\text{obs}}^\nu}, \quad (15)$$

where the subscripts ‘e’ and ‘obs’ refer to the emitter and the observer, respectively.

Because of our assumption of asymptotic flatness, at the location of the observer the spacetime is Minkowski and, therefore,  $g_{tt}(r_{\text{obs}}) \rightarrow -1$ . Moreover, because we are considering a static observer, its 4-velocity is  $u_{\text{obs}}^\mu = (1, 0, 0, 0)$ , and the denominator of the fraction in equation (15) is equal to  $-\varepsilon_p$ . The 4-velocity of the emitting particle is given by relations (7)-(10), which after inserting into equation (15) leads to

$$z = -\frac{\epsilon}{r} \sqrt{-\frac{1}{2} \frac{dg_{tt}^{(2)}}{d \ln r} \frac{l_p}{\varepsilon_p}} + \frac{\epsilon^2}{2} \left( g_{tt}^{(2)} - \frac{1}{2} \frac{dg_{tt}^{(2)}}{d \ln r} \right) + \mathcal{O}(\epsilon^3). \quad (16)$$

In this expression, we have dropped the subscripts ‘e’ and ‘obs’ for the emitter and the observer. It is implicitly understood, however, that the redshift  $z$  is measured at the location of the observer, whereas all the quantities in the right-hand side of the expression are evaluated at the location of the emitter. This expression is identical at this order to similar calculations based on different assumptions [9].

In order to calculate the quantity  $l_p/\varepsilon_p$ , we first discuss the orientation and geometry of the galaxy, the observer, and the photon trajectories in flat spacetime. All corrections due to lensing appear as factors of at least order  $\mathcal{O}(\epsilon^3)$ , which is beyond the order we are considering here.

## C. The Trajectories of Photons

We first set a coordinate system (see Fig. 1) with its origin at the center of the galaxy and oriented in such a way that the orbits of the emitting particles lie on the  $x-y$  plane. The detector of the observer defines a second plane (the image plane) at some great distance  $D$  and at an angle  $\vartheta_{\text{obs}}$  with respect to the direction of the angular momentum of the galaxy  $z$ . We use the axisymmetry of the galaxy to choose the orientation of the  $x-y$  axis so that the center of the image plane of the distant observer lies on the  $y-z$  plane.

We then set a new coordinate system (indicated by primed quantities) by rotating the original coordinate system around the  $x$ -axis by angle  $\vartheta_{\text{obs}}$ . The  $x'-y'$  plane of the new coordinate system is parallel to the image plane and the unit vector to the image plane is parallel to the  $z'$  axis

$$\hat{z}' = \begin{pmatrix} 0 \\ \sin \vartheta_{\text{obs}} \\ \cos \vartheta_{\text{obs}} \end{pmatrix}. \quad (17)$$

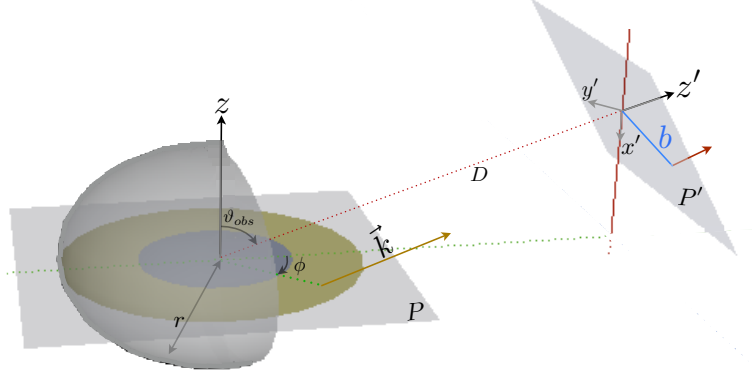


FIG. 1: A geometric representation of the galactic disk (grey) plane  $P$ . Photons with momentum  $\vec{k}$  are emitted within a ring (dark yellow) about the galactic center and arrive to the observer's image plane  $P'$  with impact parameter  $b$ . The image plane is at some distance  $D$  from the galactic plane, at an angle  $\vartheta_{\text{obs}}$  with respect to the axis of symmetry.

Coordinates on the image plane and coordinates on the galaxy plane are related via the rotation

$$\begin{pmatrix} x' \\ y' \\ z' \end{pmatrix} = \begin{pmatrix} 1 & 0 & 0 \\ 0 & \cos \vartheta_{\text{obs}} & -\sin \vartheta_{\text{obs}} \\ 0 & \sin \vartheta_{\text{obs}} & \cos \vartheta_{\text{obs}} \end{pmatrix} \begin{pmatrix} x \\ y \\ z \end{pmatrix}. \quad (18)$$

For an emitter in a circular orbit on the galactic plane at a radius  $r_e$  and at an azimuth  $\phi_e$  with respect to the  $x$ -axis, this relation becomes

$$\begin{pmatrix} x' \\ y' \\ z' \end{pmatrix} = \begin{pmatrix} 1 & 0 & 0 \\ 0 & \cos \vartheta_{\text{obs}} & -\sin \vartheta_{\text{obs}} \\ 0 & \sin \vartheta_{\text{obs}} & \cos \vartheta_{\text{obs}} \end{pmatrix} \begin{pmatrix} r_e \cos \phi_e \\ r_e \sin \phi_e \\ 0 \end{pmatrix} = \begin{pmatrix} r_e \cos \phi_e \\ r_e \cos \vartheta_{\text{obs}} \sin \phi_e \\ r_e \sin \vartheta_{\text{obs}} \sin \phi_e \end{pmatrix} \quad (19)$$

If we do not consider the bending of the trajectory of a photon due to gravitational lensing, then the  $x'$  and  $y'$  coordinates calculated with the last relation will correspond to the location on the image plane where the photon emitted by the orbiting object will be detected. The impact parameter of that photon will, therefore, be equal to

$$b = (x'^2 + y'^2)^{1/2} = r_e \sqrt{1 - \sin^2 \vartheta_{\text{obs}} \sin^2 \phi_e}. \quad (20)$$

For a photon with wave vector  $\vec{k}$  to intersect the image plane at a right angle and with an impact parameter  $b$  we require  $\hat{k} \parallel \hat{z}'$ , so  $\vec{k} = |k| \hat{z}' = |k| (\sin \vartheta_{\text{obs}} \hat{y} + \cos \vartheta_{\text{obs}} \hat{z})$ . In spherical polar coordinates, for a photon emitted in the plane  $\theta = \frac{\pi}{2}$ , the transformation from cartesian to polar is straightforward and gives

$$\vec{k} = |k| \left( \sin \vartheta_{\text{obs}} \sin \phi_e \hat{r} + \cos \vartheta_{\text{obs}} \hat{\theta} + \sin \vartheta_{\text{obs}} \cos \phi_e \hat{\phi} \right). \quad (21)$$

The null property of the photon 4-momentum requires

$$|k| = \varepsilon_p + \mathcal{O}(\epsilon^2) \quad (22)$$

which leads to

$$\frac{l_p}{\varepsilon_p} = r_e \cos \phi_e + \mathcal{O}(\epsilon^2). \quad (23)$$

#### D. Relativistic Redshifts Due to Galactic Rotation

We are now in position to calculate the Doppler shift for an axisymmetric potential and examine the properties particular to our study of galaxies. From equation (16) and (23) we write

$$z = \epsilon z_1 \sin \vartheta_{\text{obs}} \cos \phi_e + \epsilon^2 z_2 + \dots, \quad (24)$$

where

$$z_1 = -\sqrt{-\frac{1}{2} \frac{dg_{tt}^{(2)}}{d \ln r}} , \quad (25)$$

$$z_2 = \frac{1}{2} \left( g_{tt}^{(2)} - \frac{1}{2} \frac{dg_{tt}^{(2)}}{d \ln r} \right) . \quad (26)$$

Combining the first two orders, we find

$$z_2 = \frac{1}{2} \left( z_1^2 + g_{tt}^{(2)} \right) . \quad (27)$$

This last relation expresses simply the fact that the second-order energy shift has two distinct contributions: one from the second order special-relativistic Doppler shift (captured by the first term in the above sum) and one from the gravitational redshift (captured by the second term in the above sum).

In a Schwarzschild spacetime, the expressions for the Doppler shift plus redshift to all orders become

$$z_1 = - \left[ \frac{GM}{r_c c^2} \right]^{1/2} \quad (28)$$

$$z_2 = \frac{3GM}{2r_c c^2} , \quad (29)$$

where we introduced appropriate powers of the speed of light  $c$  for completeness. Because the Schwarzschild spacetime has a single scale, the relation between the first- and second-order terms is the quadratic

$$z_2 = \frac{3}{2} z_1^2 \quad (30)$$

and second-order effects are always suppressed compared to the first-order effects.

Observations [10] suggest that, to leading order, the velocity profiles of galaxies are very nearly flat over the radii of interest, i.e.,

$$z_1 = - \left( \frac{u_0}{c} \right) \left( \frac{r_0}{r} \right)^\alpha , \quad (31)$$

where  $u_0$  is the inferred, nearly constant rotational velocity, at a characteristic length scale  $r_0$  and we have introduced the small parameter  $\alpha \simeq 0$  to describe weak deviations from a constant velocity profile. Such a rotation law implies that the spacetime of the galaxy is described, to leading order, by

$$g_{tt}^{(2)} = \left( \frac{u_0}{c} \right)^2 \left\{ \begin{array}{ll} \frac{1}{\alpha} \left( \frac{r_0}{r} \right)^{2\alpha} , & \text{if } \alpha > 0 \\ \ln \left( \frac{r_{\text{out}}}{r} \right) , & \text{if } \alpha = 0 \end{array} \right. . \quad (32)$$

In this last expression for the special case  $\alpha = 0$ , we have introduced as an integration constant the radius  $r_{\text{out}} \gg r$  at which the correction term  $g_{tt}^{(2)}$  drops rapidly to zero. If a dark matter halo with a density profile  $\rho \sim r^{-2}$  is responsible for the flat rotation curve of a galaxy, then  $r_{\text{out}}$  is the outer cut-off of the halo, which is necessary for the total mass of the halo to be finite. The exact value of this constant does not affect the calculation of the redshift to first order.

Using equation (32) for the  $tt$ -element of the metric, we now calculate the next order correction to the redshift as

$$z_2 = \left( \frac{u_0}{c} \right)^2 \left\{ \begin{array}{ll} \frac{1+\alpha}{2\alpha} \left( \frac{r}{r_0} \right)^{-2\alpha} , & \text{if } \alpha < 0 \\ \frac{1}{2} - \ln \sqrt{\frac{r_{\text{out}}}{r}} , & \text{if } \alpha = 0 \end{array} \right. . \quad (33)$$

For the case of a perfectly flat rotation curve (i.e.,  $\alpha = 0$ ), the sign and magnitude of the second-order wavelength shift  $z_2$  depends explicitly on the cut-off radius  $r_{\text{out}}$ . To avoid the additional complications introduced by the presence of the cut-off radius, hereafter, we will assume  $\alpha \neq 0$  and not discuss any longer the singular case of a perfectly flat rotation curve. Surprisingly, the second-order effects can become significant for sufficiently flat rotation curves (i.e., when  $\alpha \approx 0$ ). Formally speaking, our expansion is valid only for  $\alpha \gtrsim u_0/c$ .

Note that the relation between the first- and second-order effects for a galaxy with a nearly flat rotation curve is

$$z_2 = \frac{1+\alpha}{2\alpha} z_1^2 \simeq \frac{1}{2\alpha} z_1^2 . \quad (34)$$

Equations (7), (10), (32), and (33) represent the main result of the last two sections; that both the velocity profile of matter and the gravitational and Doppler redshifts experienced by photons depend only on the same two local properties of the metric at the place of emission: the value of its  $tt$ -element and its radial derivative. Neither of the two quantities depend on the field equations of the theory of gravity, i.e., of the equation that determines the metric elements given a distribution of matter.

### III. DOPPLER AND GRAVITATIONAL CORRECTIONS TO THE LINE PROFILES

We now examine the implications of the results derived in the previous section for the atomic line profiles detected from galaxies. The flux an observer detects at a great distance  $D$  is proportional to the integral over the image plane of the specific intensity of rays that arrive perpendicular to the image plane, i.e.,

$$F_\varepsilon(\varepsilon) = \frac{1}{D^2} \int dx' \int dy' I_\varepsilon(\varepsilon) .x \quad (35)$$

Using the system of equations (19) we convert this integral into one over coordinates in the galactic plane

$$F_\varepsilon(\varepsilon) = \frac{\cos \vartheta_{\text{obs}}}{D^2} \int r_e dr_e \int d\phi_e I_\varepsilon(\varepsilon_e, r_e, \phi_e) \left( \frac{\varepsilon}{\varepsilon_e} \right)^3 , \quad (36)$$

where we have used the invariance of the quantity  $I_\varepsilon/\varepsilon^3$  to relate the intensity at arrival to that at emission by

$$I_\varepsilon(\varepsilon) = I_{\varepsilon_e}(\varepsilon_e) \left( \frac{\varepsilon}{\varepsilon_e} \right)^3 . \quad (37)$$

The observed energy  $\varepsilon$  and the emitted energy  $\varepsilon_e$  are related by the redshift relations derived in the previous section

$$\frac{\varepsilon_e}{\varepsilon} = 1 + z(r_e, \phi_e) = 1 + z_1(r_e) \sin \vartheta_{\text{obs}} \cos \phi_e + z_2(r_e) , \quad (38)$$

where we have explicitly denoted the dependence of the redshift experienced by each photon on the location of its emission.

We now assume that the emission at the local Lorentz frame is mono-energetic, at a rest-frame energy  $\varepsilon_0$ . In other words, we assume that

$$I_{\varepsilon_e}(\varepsilon_e, r_e, \phi_e) = \mathcal{I}(r_e, \phi_e) \delta[\varepsilon_e(r_e, \phi_e) - \varepsilon_0] = \mathcal{I}(r_e, \phi_e) \delta\{\varepsilon[1 + z(r_e, \phi_e)] - \varepsilon_0\} . \quad (39)$$

The flux integral, therefore, becomes

$$F_\varepsilon(\varepsilon) = \frac{\cos \vartheta_{\text{obs}}}{D^2} \int dr_e r_e \int d\phi_e \mathcal{I}(r_e, \phi_e) \delta\left\{\varepsilon - \varepsilon_0 [1 + z(r_e, \phi_e)]^{-1}\right\} [1 + z(r_e, \phi_e)]^{-3} , \quad (40)$$

where we have made a change of variables in the  $\delta$ -function to reflect the fact that the right-hand side of this equation is a flux density in the observed energy  $\varepsilon$ . We use the  $\delta$ -function to evaluate the integral over  $\phi_e$  using the relation

$$\delta[g(\phi)] = \delta(\phi) \sum_i \left| \frac{dg}{d\phi} \right|_{\phi_i}^{-1} , \quad (41)$$

where  $\phi_i$  is each solution to the equation  $g(\phi_i) = 0$  or, in our case,

$$g(\phi_i) = 0 \Rightarrow \varepsilon - \varepsilon_0 [1 + z(r_e, \phi_i)]^{-1} = 0 . \quad (42)$$

Using the expression (24) for the redshift, we obtain

$$\cos \phi_i = \frac{1}{z_1 \sin \vartheta_{\text{obs}}} \left( \frac{\varepsilon_0}{\varepsilon} - 1 - z_2 \right) , \quad (43)$$

which leads to two solutions for the angle  $\phi_i$  with opposite signs. Requiring that  $|\cos \phi_i| \leq 1$  allows us to place limits on the range of photon energies that contribute to the line as

$$\left( \frac{\varepsilon_\pm}{\varepsilon_0} \right) = \frac{1}{1 \pm z_1 \sin \vartheta_{\text{obs}} + z_2} . \quad (44)$$

In evaluating the integral, we also need the derivative

$$\left| \frac{dz}{d\phi_e} \right|_{\phi_e=\phi_i} = \left[ z_1^2 \sin^2 \vartheta_{\text{obs}} - \left( \frac{\varepsilon_0 - \varepsilon}{\varepsilon} \right)^2 + 2 \left( \frac{\varepsilon_0 - \varepsilon}{\varepsilon} \right) z_2 \right]^{1/2}. \quad (45)$$

Using the above expressions, the flux becomes

$$\begin{aligned} F_\varepsilon(\varepsilon) &= \frac{\cos \vartheta_{\text{obs}}}{D^2} \int dr_e r_e \sum_i \mathcal{I}(r_e, \phi_i) [1 + z(r_e, \phi_i)]^{-3} \left| \frac{dg}{d\phi_e} \right|_{\phi_e=\phi_i}^{-1} \\ &= 2 \frac{\cos \vartheta_{\text{obs}}}{D^2} \int dr_e r_e [1 + z(r_e, \phi_i)]^{-1} \left| \frac{dz}{d\phi_e} \right|_{\phi_e=\phi_i}^{-1} \left[ \frac{\mathcal{I}(r_e, \phi_i) + \mathcal{I}(r_e, -\phi_i)}{2} \right] \\ &= 2 \frac{\cos \vartheta_{\text{obs}}}{D^2} \left( \frac{\varepsilon}{\varepsilon_0} \right) \int dr_e r_e \left| \frac{dz}{d\phi_e} \right|_{\phi_e=\phi_i}^{-1} \left[ \frac{\mathcal{I}(r_e, \phi_i) + \mathcal{I}(r_e, -\phi_i)}{2} \right] \\ &\simeq 2 \frac{\cos \vartheta_{\text{obs}}}{D^2} \left( \frac{\varepsilon}{\varepsilon_0} \right) \int dr_e r_e \left[ z_1^2 \sin^2 \vartheta_{\text{obs}} - \left( \frac{\varepsilon_0 - \varepsilon}{\varepsilon} \right)^2 + 2 \left( \frac{\varepsilon_0 - \varepsilon}{\varepsilon} \right) z_2 \right]^{-1/2} \left[ \frac{\mathcal{I}(r_e, \phi_i) + \mathcal{I}(r_e, -\phi_i)}{2} \right]. \end{aligned} \quad (46)$$

To explore the properties of the second-order corrections to the line profiles, we make for now the simplifying assumption that the emission comes from a single annulus in the galactic disk with intensity that is independent of azimuth, at a radius  $r_0$  and with a width  $\delta r$ . In this case, the line profile becomes

$$F_\varepsilon(\varepsilon) = 2 \cos \vartheta_{\text{obs}} \mathcal{I}(r_0) \left( \frac{r_0 \delta r}{D^2} \right) \left( \frac{\varepsilon}{\varepsilon_0} \right) \left[ z_1^2 \sin^2 \vartheta_{\text{obs}} - \left( \frac{\varepsilon_0 - \varepsilon}{\varepsilon} \right)^2 + 2 \left( \frac{\varepsilon_0 - \varepsilon}{\varepsilon} \right) z_2 \right]^{-1/2}, \quad (47)$$

which we express in terms of the dimensionless quantity

$$\begin{aligned} \mathcal{F}_\varepsilon &\equiv \frac{F_\varepsilon(\varepsilon)}{2 \cos \vartheta_{\text{obs}} \mathcal{I}(r_0)} \left( \frac{r_0 \delta r}{D^2} \right)^{-1} \\ &= \left( \frac{\varepsilon}{\varepsilon_0} \right) \left[ z_1^2 \sin^2 \vartheta_{\text{obs}} - \left( \frac{\varepsilon_0 - \varepsilon}{\varepsilon} \right)^2 + 2 \left( \frac{\varepsilon_0 - \varepsilon}{\varepsilon} \right) z_2 \right]^{-1/2}, \end{aligned} \quad (48)$$

The minimum and maximum photon energies for which the flux is non-zero are given by equation (44). Because of the second-order Doppler shifts and the gravitational redshift, the center of the broadened profile is displaced from the rest energy of the line by an amount equal to

$$\bar{\varepsilon} = \frac{1}{2} (\varepsilon_- + \varepsilon_+) = \varepsilon_0 (1 + z_1^2 \sin^2 \vartheta_{\text{obs}} - z_2). \quad (49)$$

Moreover, the amplitude of the red wing of the line is smaller than the amplitude of the blue wing.

Figures (2) and (3) show the dimensionless line profiles from narrow annuli in a Schwarzschild spacetime and in the spacetime of a galaxy with a nearly flat rotation curve, for different values of the parameters  $z_1$  and  $\alpha$  (see equation [30] and [34]) and for different inclinations of the observer. In the case of a galaxy with a nearly flat rotation curve, the broadened line is gravitationally redshifted by an amount that is larger compared to the equivalent Schwarzschild case. If the flat rotation curve is a result of a dark matter halo, the additional redshift occurs because the dark matter halo has a density profile  $\rho \simeq r^{-2}$  and a large amount of mass (and hence of gravitational redshift) exists outside the location of the annulus. If this second-order effect is not corrected for, it will be assigned to the overall recession velocity of the galaxy  $V_g$  that is due to its peculiar motion and to the Hubble flow. The error is, nevertheless, small as it is of order

$$\begin{aligned} \left| \frac{\delta V_g}{V_g} \right| &\simeq \left| \frac{\bar{\varepsilon} - \varepsilon_0}{\varepsilon_0} \right| = \left| \sin^2 \vartheta_{\text{obs}} - \frac{1 + \alpha}{2\alpha} \right| z_1^2 \\ &\simeq \frac{1}{2\alpha} \left( \frac{V_{\text{rot}}}{c} \right)^2 = \frac{1}{2} \left( \frac{V_{\text{rot}}}{\alpha c} \right) \left( \frac{V_{\text{rot}}}{c} \right) \leq \frac{1}{2} \left( \frac{V_{\text{rot}}}{c} \right) \ll 1 \quad \text{when } \alpha \geq \frac{V_{\text{rot}}}{c}, \end{aligned} \quad (50)$$

where  $V_{\text{rot}}$  is the inferred rotational velocity from the non-relativistic Doppler shift.

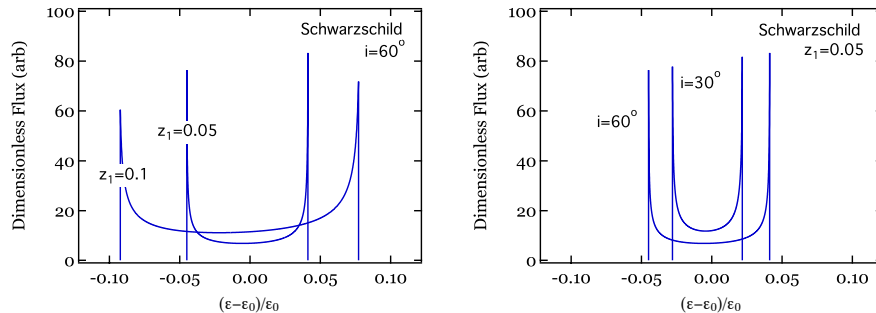


FIG. 2: Profiles of broadened atomic lines that originate in an annulus in a Schwarzschild spacetime for different values of the non-relativistic Doppler shift  $z_1$  and inclinations of the observer. The overall effect of the relativistic Doppler shift and of the gravitational redshift is to make the profile asymmetric and to shift it towards lower energies.

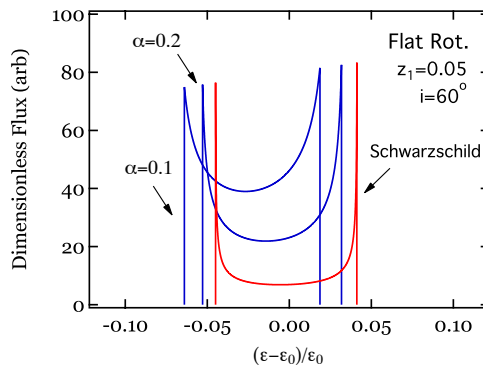


FIG. 3: Profiles of broadened atomic lines that originate in an annulus in a galactic disk plotted for different values of the parameter  $\alpha$ , which measures the degree of flatness of the galactic rotation curve. The red line shows, for comparison, the line in a Schwarzschild spacetime with the same amount of non-relativistic Doppler shift. The spacetime that corresponds to a flat rotation curve leads to a larger overall redshift as well as to less pronounced blue and red wings for the line. Note that the parameter  $z_1$  used for this plot is unphysically large for a galaxy and was chosen here in order to make the effect visible.

#### IV. A STATISTICAL MEASURE OF THE RELATIVISTIC DOPPLER SHIFT AND OF THE GRAVITATIONAL REDSHIFT

In the previous section, we calculated the profile of an atomic line that originates in the equatorial plane of a galaxy in a general metric theory of gravity. We showed that the non-relativistic Doppler shift, the relativistic (i.e., second-order) Doppler shift, and the gravitational redshift experienced by a photon from its origin to a distant observer depend on the magnitude and local radial derivative of the  $tt$ -element of the metric,  $g_{tt}$ , at its origin. We derive here quantities that enable the measurement of these second-order corrections.

We start by considering a single galaxy at a redshift  $z_g$ , which accounts for both the peculiar velocity of the galaxy as well as the Hubble flow. We will assume that the rotational profile of the galaxy, as inferred from non-relativistic Doppler shifts, is nearly flat and described by equation (31) from some inner radius  $r_0$  to an outer radius  $\gg r_0$ , i.e.,

$$z_1 = - \left( \frac{u_0}{c} \right) \left( \frac{r}{r_0} \right)^{-\alpha}. \quad (51)$$

The relativistic Doppler shift and the gravitational redshift introduce an additional overall change in the energy of the photon that we described by the quantity  $z_2$  given, in general, by equation (27). If photons and particles follow geodesics in the same spacetime, i.e., if the theory of gravity obeys the equivalence principle, then the gravitational redshift can be calculated using the same metric that determines the velocities of the emitting hydrogen atoms. In this case,  $z_2$  is related to  $z_1$  according to equation (34). If, on the other hand, the theory of gravity does not obey the equivalence principle, then the amount of gravitational redshift experienced by each photon will not have the same relation to the non-relativistic Doppler shifts. We parametrize the possibility of the theory not obeying the



equivalence principle by the single constant  $f$  and write, in general, the second-order energy shift as

$$z_2 = \frac{f + \alpha}{2\alpha} z_1^2. \quad (52)$$

For a gravity theory that obeys the equivalence principle,  $f \equiv 1$ .

The line profile measured by an observer at infinity will extend between the two energies  $\varepsilon_-$  and  $\varepsilon_+$  dominated by the largest rotational velocities and, therefore, (see eq. [44])

$$\varepsilon_{\pm} = \frac{\varepsilon_0}{1 + z_g} \left[ 1 \pm \left( \frac{u_0}{c} \right) \sin \vartheta_{\text{obs}} + \left( \frac{u_0}{c} \right)^2 \left( \sin^2 \vartheta_{\text{obs}} - \frac{f + \alpha}{2\alpha} \right) \right]. \quad (53)$$

The width of the line is

$$\Delta\varepsilon \equiv \varepsilon_+ - \varepsilon_- = \frac{\varepsilon_0}{1 + z_g} \left[ 2 \left( \frac{u_0}{c} \right) \sin \vartheta_{\text{obs}} \right] \quad (54)$$

and is determined by the non-relativistic Doppler shift. On the other hand, the center of the line is

$$\bar{\varepsilon} \equiv \frac{1}{2} (\varepsilon_+ + \varepsilon_-) = \frac{\varepsilon_0}{1 + z_g} \left[ 1 + \left( \frac{u_0}{c} \right)^2 \left( \sin^2 \vartheta_{\text{obs}} - \frac{f + \alpha}{2\alpha} \right) \right] \quad (55)$$

and deviates from  $\varepsilon_0/(1 + z_g)$  by second order effects. These two gross properties of the line profile depend on four parameters of the galaxy and on the gravitational theory: the redshift of the galaxy  $z_g$ , its rotational velocity  $u_0$ , the inclination of the observer  $\vartheta_{\text{obs}}$ , and the ratio  $f/\alpha$ . In principle, we can perform an independent measurement of the redshift  $z_g$  of the galaxy using optical lines from the galactic nucleus. For a sufficiently large sample of galaxies, we may also use a statistical argument regarding the distribution of inclinations. Hence we can use precise measurements of both  $\Delta\varepsilon$  and  $\bar{\varepsilon}$  for a large number of galaxies in order to measure statistically the parameter  $f/\alpha$  and, hence, constrain deviations from the equivalence principle.

Because the above argument is of a statistical nature, it will be difficult to determine the formal and, more importantly, the systematic uncertainties of the result based solely on this single type of measurement. There is, however, an additional measurable quantity that provides an independent measure of the same parameters and can be used as a consistency check in case any deviations from the equivalence principle are found. The relativistic-Doppler shift and the gravitational redshift not only introduce an additional energy shift to the line, but also make it asymmetric, with the blue wing appearing brighter than the red wing. As a result, we obtain an independent third observable from each galaxy in the flux averaged photon energy

$$\langle \varepsilon \rangle \equiv \frac{\int d\varepsilon \varepsilon F_\varepsilon(\varepsilon)}{\int d\varepsilon F_\varepsilon(\varepsilon)}. \quad (56)$$

For a symmetric line,  $\langle \varepsilon \rangle = \bar{\varepsilon}$ ; any correction to this equality will be due to the second-order relativistic effects.

For simplicity, we first perform the calculation of  $\langle \varepsilon \rangle$  in the frame of the galaxy and add the redshift due to the Hubble flow and its peculiar velocity only in the final result. In deriving the flux averaged photon energy, we need to evaluate two integrals of the form (see eq. [46])

$$\begin{aligned} E_n &= \int d\varepsilon \varepsilon^n F_\varepsilon(\varepsilon) \\ &= 2 \frac{\cos \vartheta_{\text{obs}}}{D^2} \int dr_e r_e \int d\varepsilon \varepsilon^n [1 + z(r_e, \phi_i)]^{-1} \left| \frac{dz}{d\phi_e} \right|_{\phi_e=\phi_i}^{-1} \left[ \frac{\mathcal{I}(r_e, \phi_i) + \mathcal{I}(r_e, -\phi_i)}{2} \right]. \end{aligned} \quad (57)$$

We write

$$\varepsilon = \varepsilon_0 \frac{1}{1 + z(r_e, \phi_i)} \quad (58)$$

and make the change of variables from  $\varepsilon$  to  $\phi_i$

$$d\varepsilon = -\varepsilon_0 \left[ \frac{1}{1 + z(r_e, \phi_i)} \right]^2 \frac{dz}{d\phi_e} \Big|_{\phi_e=\phi_i} d\phi_i. \quad (59)$$

As a result, the general expression for each integral becomes

$$\begin{aligned}
E_n &= 2\varepsilon_0^n \frac{\cos \vartheta_{\text{obs}}}{D^2} \int dr_e r_e \int_0^\pi d\phi_i [1 + z(r_e, \phi_i)]^{-3-n} \left[ \frac{\mathcal{I}(r_e, \phi_i) + \mathcal{I}(r_e, -\phi_i)}{2} \right] \\
&\simeq \varepsilon_0^n \frac{\cos \vartheta_{\text{obs}}}{D^2} \int dr_e r_e \int_0^{2\pi} d\phi_i \mathcal{I}(r_e, \phi_i) [1 + z_1 \sin \vartheta_{\text{obs}} \cos \phi_i + z_2]^{-3-n} \\
&\simeq \varepsilon_0^n \frac{\cos \vartheta_{\text{obs}}}{D^2} \int r_e dr_e d\phi_i \mathcal{I}(r_e, \phi_i) \left\{ 1 - (3+n) \left[ z_1 \sin \vartheta_{\text{obs}} \cos \phi_i + z_2 - \frac{(4+n)}{2} z_1^2 \sin^2 \vartheta_{\text{obs}} \cos^2 \phi_i \right] \right\}. \quad (60)
\end{aligned}$$

Inserting first the general relation (52) between the first- and second-order energy shifts, we obtain

$$\begin{aligned}
E_n &= \varepsilon_0^n \frac{\cos \vartheta_{\text{obs}}}{D^2} \left\{ \int r_e dr_e d\phi_i \mathcal{I}(r_e, \phi_i) + (3+n) \left[ \frac{(4+n)}{2} \sin^2 \vartheta_{\text{obs}} \int r_e dr_e d\phi_i \mathcal{I}(r_e, \phi_i) z_1^2 \cos^2 \phi_i \right. \right. \\
&\quad \left. \left. - \left( \frac{f+\alpha}{2\alpha} \right) \int r_e dr_e d\phi_i \mathcal{I}(r_e, \phi_i) z_1^2 - \sin \vartheta_{\text{obs}} \int r_e dr_e d\phi_i \mathcal{I}(r_e, \phi_i) z_1 \cos \phi_i \right] \right\}. \quad (61)
\end{aligned}$$

We now write this expression more compactly by defining an intensity average of quantities involving  $z_1$  and  $\cos \phi_i$  as follows

$$\langle z_1^\alpha \cos^\beta \phi_i \rangle = \frac{\int r_e dr_e d\phi_i \mathcal{I}(r_e, \phi_i) z_1^\alpha \cos^\beta \phi_i}{\int r_e dr_e d\phi_i \mathcal{I}(r_e, \phi_i)} \quad (62)$$

The flux averaged photon energy is then given by

$$\langle \varepsilon \rangle = \frac{E_1}{E_0} = \frac{\varepsilon_0}{1 + z_g} \left[ 1 - \sin \vartheta_{\text{obs}} \langle z_1 \cos \phi \rangle + 9 \sin^2 \vartheta_{\text{obs}} \langle z_1 \cos \phi \rangle^2 + 4 \sin^2 \vartheta_{\text{obs}} \langle z_1^2 \cos^2 \phi \rangle - \frac{f+\alpha}{2\alpha} \langle z_1^2 \rangle \right]. \quad (63)$$

The fluxed average photon energy in each galaxy depends strongly on the degree of asymmetry in the emission. However, we can again make a statistical measurement of the parameter  $f/\alpha$  using a large sample of galaxies. Indeed, because the angle  $\phi_i$  is measured with respect to the distant observer, its values for different galaxies will not be correlated with the first-order redshift  $z_1$  but will be randomly distributed. As a result, in a statistical sense, equation (63), when averaged over all possible azimuthal orientations of the observer, will be

$$\langle \varepsilon \rangle = \frac{E_1}{E_0} = \frac{\varepsilon_0}{1 + z_g} \left[ 1 + \left( \frac{u_0}{c} \right)^2 \left( 2 \sin^2 \vartheta_{\text{obs}} - \frac{f+\alpha}{2\alpha} \right) \right], \quad (64)$$

where we have also taken advantage of the slow variation of  $z_1$  with radius  $r_e$ . When combined with equation (54) for the width of the line and averaged over all possible inclinations of the observer  $\theta_{\text{obs}}$ , the flux averaged energies of a large sample of galaxies will also lead to an independent measurement of the parameter  $f/\alpha$  and hence to a test of the equivalence principle.

## V. DISCUSSION

In this article, we calculated the second-order special relativistic and gravitational effects on the rotationally broadened line profiles from galaxies. We identified two measurable quantities (eqs. [55] and [64]), which can be used in conjunction with the observed line widths (eq. [54]) to test the validity of the equivalence principle at galactic scales.

The level at which we can perform this test depends on the formal uncertainties in each measurement, as well as on the degree of azimuthal symmetry in the emission of each galaxy, which can mask the asymmetry in the line profile due to relativistic effects. To estimate the magnitude of these two sources of uncertainty, we examine some HI profiles provided as results of ongoing single beam surveys [11].

As evident from Fig. 4, line profiles for individual galaxies, even when they are of high signal-to-noise and sharply double peaked, can have morphologies quite different from the azimuthally symmetric case of Fig. 3. This variance is because the HI is not necessarily smoothly distributed and galaxies often are lopsided in the stellar or gaseous distribution [12]. Therefore, even if the effect we are searching for is large, which it is not, the nature of this measurement must be statistical.

We also estimate the internal uncertainties using an estimate of the spectral noise from regions outside of the profile and 1000 simulations with noise added to the spectra. Because this noise is superposed on the original spectrum, the

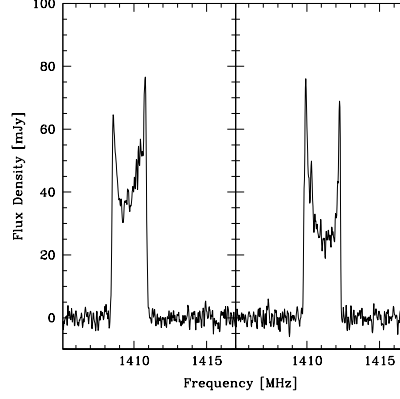


FIG. 4: HI profiles of two massive galaxies ( $V_{\text{rot}} > 200$  km/sec) that are among those with the highest signal-to-noise ratio in the sample. The two profiles show different signs of the asymmetry, reflecting the “noise” introduced in such measurements by the internal, structural asymmetries of the galaxies.

noise of the simulations is actually  $\sqrt{2}$  larger, resulting in a slight overestimate of the internal uncertainties. We find that these are always smaller than the systematic errors due to intrinsic profile asymmetries.

A precision measurement of the parameter  $f$ , which measures potential violations of the equivalence principle, requires great care in handling of the data as subtle biases can be introduced by careless binning or scaling. While we argued earlier that we could average over a suitably large distribution of inclinations, it is, in principle, possible to obtain independent measurements of the inclinations of individual galaxies which would further restrict the range of the constraints. New surveys will be releasing many thousands of galaxy spectra in the near future, which offers the possibility of placing constraints on potential equivalence principle violations on the scale of galaxies. We will discuss a detailed observational strategy for dealing with these issues in a forthcoming article.

### Acknowledgments

We thank Feryal Özel for useful discussions. This work was supported in part by the NSF CAREER award NSF 0746549 to DP and NSF AST-0907771 to DZ.

- 
- [1] D. Zaritsky & S.D.M. White *Astrophys. J.* **435** 599 (1994); T. G. Brainerd, R.D., Blandford, & I. Smail *Astrophys. J.* **466** 623 (1996)
  - [2] see, e.g., E. Armengaud, C. Augier, A. Benoît, et al. *Phys. Let. B* **687**, 294 (2010); E. Aprile, K. Arisaka, F. Arneodo, F., et al. *Phys. Rev. Lett.* **107**, 131302 (2011); Ahmed Z. et al. *Phys. Rev. Lett.* **106** 131302 (2011); Angloher, G. et al. 2011, arXiv:1109.0702;
  - [3] M. Milgrom *Astrophys. J.* **270**, 384 (1983); *Astrophys. J.* **270**, 371 (1983); *Astrophys. J.* **270**, 365 (1983)
  - [4] R. H. Sanders, R. H., & S. S. McGaugh *ARAA* **40**, 263 (2002)
  - [5] see, e.g., J. Bekenstein, & M. Milgrom, *Astrophys. J.* **286**, 7 (1984); P. D. Mannheim, & D. Kazanas, *Astrophys. J.* **342**, 635 (1989); J. D. Bekenstein, & R. H. Sanders, *Astrophys. J.* **429**, 480 (1994); R. H. Sanders *Astrophys. J.* **480**, 492 (1997)
  - [6] J. D. Bekenstein, & R. H. Sanders, *R. H. EAS Pub. Ser.* **20**, 225 (2006); J. D. Bekenstein, *Phys. Rev. D* **70**, 083509 (2004); M. Milgrom *Phys. Rev. D* **80**, 123536 (2009); L. Blanchet, & S. Marsat, *Phys. Rev. D* **84**, 044056 (2011); C. Deffayet, G. Esposito-Farese, & R. P. Woodard arXiv:1106.4984 (2011).
  - [7] M. Milgrom *Annals of Physics* **229**, 384 (1994); *Phys. Let. A* **253**, 273 (1999); *New Astr. Rev.* **46**, 741 (2002)
  - [8] M. Kesden, & M. Kamionkowski *Phys. Rev. D* **74**, 083007 (2006); *Phys. Rev. Lett.* **97** 131303
  - [9] K. Lake, *Phys. Rev. Lett.* **92**, 051101; T. Faber, & M. Visser, *Mon. Not. Royal Astr. Soc.* **372**, 136 (2006)
  - [10] Y. Sofue, & V. Rubin *ARAA* **39**, 137 (2001)
  - [11] R. Giovanelli et al. *Astron. J.* **133** 2569 (2007); A. Saintonge, R. Giovanelli, M. P. Haynes, L. G. Hoffman, B. R. Kent, A. M. Martin, S. Stierwalt, & N. Brosch *Astron. J.* **135** 588 (2008); B. R. Kent et al. *Astron. J.* **136** 713 2008
  - [12] J.E. Baldwin, D. Lynden-Bell, & R. Sancisi *Mon. Not. Royal Astr. Soc.* **193**, 313; H.-W. Rix & D. Zaritsky *Astrophys. J.* **447**, 82 (1995); M. P. Haynes, L. van Zee, D. Hogg, M. S. Roberts, & R. J. Maddalena *AJ*, **115**, 62 (1998)